Received: 28 February 2025 | Revised: 03 April 2025 | Accepted: 16 April 2025

DOI: https://doi.org/10.69547/NS.31.03

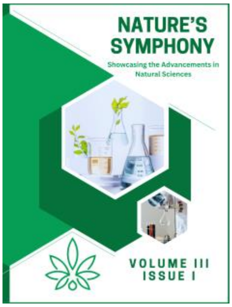

NATURE'S SYMPHONY

ISSN-E: 3007-2034

ISSN-P: 3007-2026

Website link: www.tsfns.com

Green Fabrication of ZnO Nanoparticles with *Coriandrum sativum* Leaf Extract: Investigating Catalytic and Antimicrobial Potentials

Bakhtawar Sajjad, Humayun Ajaz, Shaista Ali, Muhammad Mudassar, Atif Yaqub, Sarwar Allah Ditta, Sharafat Ali

To cite: Sajjad, B., Ajaz, H., Ali, S., Mudassar, M., Yaqoub, A., Ditta, SA., and Ali, S. 2025. Green Fabrication of ZnO Nanoparticles with *Coriandrum sativum* Leaf Extract: Investigating Catalytic and Antimicrobial Potentials. *Nature's Symphony*, 3(1):32-48.

Article QR

Published online: 02 May 2025
Submit your article to this journal: https://tsfjb.com/ojs/index.php/tsfns/about/submissions
View archive: https://tsfjb.com/ojs/index.php/tsfns/issue/archive/

Research Article

Green Fabrication of ZnO Nanoparticles with *Coriandrum sativum* Leaf Extract: Investigating Catalytic and Antimicrobial Potentials

Bakhtawar Sajjad[1] | Humayun Ajaz[1] | Shaista Ali[2*] | Muhammad Mudassar[3] | Atif Yaqoub[4] | Sarwar Allah Ditta[4] |Sharaft Ali[4]

[1]Department of Chemistry University of Engineering and Technology Lahore, Pakistan
[2]Institute of Chemical Sciences, Government College University, Lahore, Pakistan
[3]Department of Biological Sciences, Superior University, Lahore, Pakistan
[4]Department of Zoology, Government College University, Lahore, Pakistan

***Correspondence**
Shaista Ali
Email:
shaista.ali.19@gmail.com,
shaista.ali@gcu.edu.pk

Keywords:
Green Synthesis, *Coriandrum sativum* Leaves, Zinc Oxide nanoparticles, Photocatalysis, Antimicrobial Activity

ABSTRACT

Sustainable approach to synthesizing nanoparticles is a requirement now. In current research work, a sustainable green method using *Coriandrum sativum* leaf extract was used to synthesize zinc oxide (ZnO) nanoparticles. The confirmation of the synthesized product was done using Fourier transform infrared spectroscopy (FTIR), Photoluminescence (PL), UV-Visible spectroscopy, and powder X-ray Diffraction analysis. pXRD analysis showed orthorhombic structure with 1.8 nm (by Scherrer equation) and PL spectroscopy gave emission and excitation peak at 536 nm. The band gap, determined from the UV–visible absorption spectra via Tauc's plot method, was found to be approximately 3.37 eV. The photocatalytic efficiency of ZnO against methylene blue dye was found to be 82% and the antibacterial activity was found against *Staphylococcus aureus* and *Escherichia coli*. The observed negative surface charge of -2.1 mV determined by zeta potential analysis, supported these results by indicating moderate colloidal stability and electrostatic interactions. The negatively charged ZnO surface enhances adsorption of positively charged dye molecules and facilitates interaction with bacterial membranes, contributing to both photocatalytic and antibacterial effects.

1. INTRODUCTION

Water pollution has been a major issue for the last several years as it contains a large number of ions and dyes from industries. The hazards of wastewater lead scientists to solve this environmental issue. A large number of techniques like stripping, adsorption, precipitation, reverse osmosis, ultra and micro filtration have been used conventionally. These techniques may only lead to phase change of non-corroding, undecaying matter to sludge (Abdullah *et al.*, 2022) and further treatments make them costly. ZnO and TiO_2 nanoparticles (NPs) are commonly used photocatalysts because of their many properties such as high efficiency, photochemical stability, insolubility, and non-toxicity.

Semiconductor (n-type) NPs like ZnO with band gap of 3.2eV exhibits a large binding energy, i.e., 60 meV and non-toxic nature. ZnO NPs have a photodegradation mechanism similar to TiO (Weldegebrieal, 2020) which make them potential photocatalyst. Many synthesis methodologies like sol-gel (Singh *et al.*, 2021), precipitation/co-precipitation (Ahmad *et al.*, 2022), sonication, hydrothermal, and thermal decomposition methods have been used to synthesize ZnO NPs. ZnO NPs are employed in electronics, communication, sensors, cosmetics, environmental protection, biology, and medicine (Chikkanna *et al.*, 2019). ZnO band gap is split into many sub-gaps by visible light absorbance (Rueda-Marquez *et al.*, 2020; Chan *et al.*, 2021; Javed *et al.*, 2021). The efficiency of ZnO as a photocatalyst is studied when an excited electron shifts from valence to conduction band by irradiation. During this procedure, the absorbed energy (hν) from irradiation equals or sometimes exceeds the photocatalyst band gap. Many organic and inorganic pollutants can be degraded by the photogenerated electrons and holes (Khan *et al.*, 2022). Several possible reactions involve the formation of an electron hole (e^{-} - h^{+}) on the ZnO nanoparticle's surface making it a useful photocatalyst.

In recent years, green synthesis has attained great attention because it uses eco-friendly materials and avoids hazardous chemicals for synthesis in pharmaceutical and biological applications. The biological method of synthesizing metallic NPs with diverse microorganisms is greener, energy-efficient, and cheaper than the chemical ones. Biomedical applications of bio-inspired NPs are intriguing due to their biocompatibility and the NPs coated with biological molecules are biocompatible as compared to chemically produced NPs (Javed *et al.*, 2021). Agricultural wastes or plants and their parts can replace chemical synthetic operations since they do not require intracellular synthesis, purification stages, or microbial cell cultures. Phytochemical studies have shown that the plants and their metabolites include quercetin, lupeol, sitosterol, oleanolic acid, rutin, leucocyanidin, anthocyanins, proanthocyanidins and glucosides and kaempferol (Doubi *et al.*, 2022). Many researchers are working on plant based green synthesized NPs using metal oxides like Zn, Fe, Ni, Mn, but among them ZnO is of huge importance (Chan *et al.*, 2021; Javed *et al.*, 2021).

Depending on the plant extract and the experimental conditions, different photocatalytic degradation efficiencies of green-synthesized ZnO NPs have been reported in previous research. For instance, ZnO NPs made from *Phoenix roebelenii* leaves degraded methylene blue (MB) by 98% in 105 minutes when exposed to UV light (Aldeen *et al.*, 2022) whereas ZnO NPs synthesized using *Syzygium cumini* leaves achieved 91.4% MB degradation under sunlight in 180 minutes (Sadiq *et al.*, 2021). Similarly, *Acalypha indica* mediated ZnO NPs exhibited 96% degradation of MB dye in 90 min (Kamarajan *et al.*, 2022). In contrast, moderate to lower efficiencies have been reported using *Pithecellobium dulce* peel (63% in 120 min) (Madhumitha *et al.*, 2019), Broccoli extract (74% in 120 min) (Osuntokun *et al.*, 2019), and *Synadium grantii* leaves (36.5% in 75 min) (Karthik *et al.*, 2022), all under UV light. On average, reported degradation efficiencies range from 36% to 98%, influenced by the synthesis method, plant extract, and reaction conditions.

Present work includes the green synthesis of ZnO NPs and their applications in methylene blue degradation and their potential for antibacterial activity against the (Gram +ve) *Staphylococcus aureus* and (Gram -ve) *Escherichia coli*.

In present study, ZnO NPs were synthesized using *Coriandrum sativum* leaf extract, achieving 82% degradation of MB dye under UV light over 280 minutes. This demonstrates the promising photocatalytic capability of Coriandrum sativum synthesized ZnO NPs and contributes a novel, eco-friendly approach to sustainable dye degradation for wastewater treatment applications, and compatibility with biological systems, making it suitable for future biomedical and environmental applications.

2. EXPERIMENTAL

2.1 Materials and Chemicals

The fresh leaves of *Coriandrum sativum* were collected from a vegetable market located near the University of Engineering and Technology Lahore, zinc acetate dihydrate (0.01M), sodium hydroxide (2 M) was purchased from Sigma-Aldrich. All the solutions were prepared using distilled and deionized water.

2.2 Preparation of *Coriandrum sativum* Leaf Extract

Coriandrum sativum leaves were chopped finely, washed with distilled H_2O repeatedly to remove any impurities, and dried at 60 °C. Dried leaves (50 g in 200 mL distilled H_2O) were boiled till solution turned dark yellow, cooled at ambient temperature conditions and filtered with Whatman filtration paper (No.40) (Chan *et al.*, 2021).

2.3 Synthesis of Zinc Oxide Nanoparticles

About 0.2 g of zinc acetate dihydrate ($Zn(CH_3COO)_2.2H_2O$) was added into the 50 mL of distilled H_2O and then solution was rapidly agitated for 15 minutes. After that 1.0 mL *Coriandrum sativum* leaf extract was poured to the prepared solution. The pH of prepared solution was attained around 12 by adding 0.05 mL of 2 M sodium hydroxide solution every 5 minutes and pale white precipitates were obtained. The reaction was stirred for 2 hours and was centrifuged at 4000 rpm for 15 minutes and rinsed with distilled H_2O and then ethanol was used to purify the obtained product. After purification of product, the collected precipitates were calcined for 1 hour at 400 °C after being dried overnight in an oven at 60 °C (Weldegebrieal, 2020).

2.4 Photocatalytic Measurements

The photocatalytic efficiency of synthesized material was demonstrated through the breakdown of organic dye (methylene blue) under visible light illumination. 20 ppm solution of MB dye was prepared using deionized H_2O. To determine the specific wavelength at which optimum absorbance occurs, blank solution (without analyte) was run through the UV-Visible spectrophotometer. The λ_{max} of methylene blue dye was reported to be 662 nm. After running the blank, 20 mL of methylene blue solution using stock was taken in a beaker and 10 mg of prepared NPs were also added in the methylene blue solution. Then the absorbance of solution was measured after every 15 minutes at 662 nm. The obtained data was further used for the determination of catalytic potential of prepared ZnO NPs. The following equation was used to investigate or calculate the efficiency of green synthesized ZnO NPs towards the degradation of methylene blue dye (Khan *et al.*, 2022).

$$\text{Photodegradation efficiency (\%)} = C_o\text{-}C_t \,/\, C_o \times 100 \quad \textbf{(1)}$$

where C_t represents the concentration of the methylene blue with photocatalyst after irradiation at a certain time during the reaction (t) and C_o refers to the initial concentration of MB dye in the absence of photocatalyst prior to light irradiation (Haleem *et al.*, 2023; Hussain *et al.*, 2024). Numerous studies have demonstrated that the degradation of organic pollutants under light irradiation adheres to the Langmuir– Hishelwood (L–H) kinetic model as described in Eq. (2)

$$r = dA/dt = k\,(K_c /1+K_c) \quad \textbf{(2)}$$

where the reaction rate (mg/L min) is denoted by r, the reaction constant (min^{-1}) represented by k, while K is the adsorption coefficient of the reactant (L/mg) and A is the absorbance of the reactant (mg/L). When the concentration of chemical species is low, the equation reduces to a pseudo-first-order kinetic expression as shown in Eq. (3)

$$r = kKC_0 = k_{app}C_t \quad \textbf{(3)}$$

By integrating equation 3:

$$\ln (C_0/C_t) = -k_{app}\, t \qquad (4)$$

Graph plot between C_o/C_t and time (t) gives a straight-line equation, slope of a straight line is equal to the apparent first-order rate constant K_{app}.

2.5 Antimicrobial Activity of ZnO Nanoparticles

Disc diffusion method was used to determine the antimicrobial efficiency of ZnO NPs against both *Staphylococcus aureus* and *Escherichia coli.* Bacterial cultures were grown in nutrient broth at 37 °C for 24 hours. After that the agar plates were inoculated with 100 µL of the bacterial suspension, and sterile discs (6 mm) impregnated with 10–20 µL of the test sample were placed on the surface. Plates were incubated at 37 °C for 24 hours, and zones of inhibition were measured in millimeters (Altaf *et al.*, 2020).

3. RESULTS AND DISCUSSION

3.1 Fourier Transform Infrared (FTIR)

Figure 1 shows the confirmation of ZnO NPs with the capping of the functional groups present in *Coriandrum sativum* leaf extract. O-H stretching peak was observed at 3270 cm^{-1}, amine -NH vibration stretch at 1406 cm^{-1} and Zn-O stretching and vibration frequency at 1564, and 713 cm^{-1}.

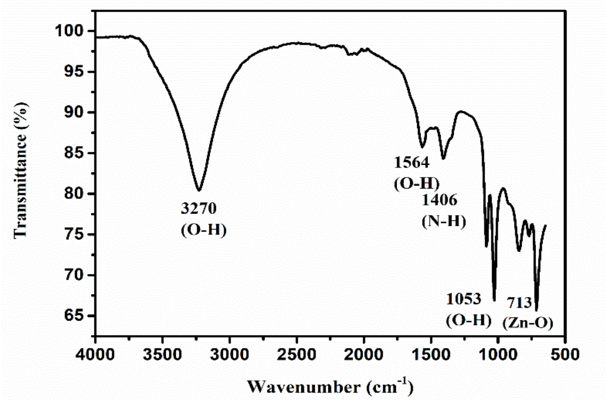

Figure 1. FTIR of ZnO nanoparticles

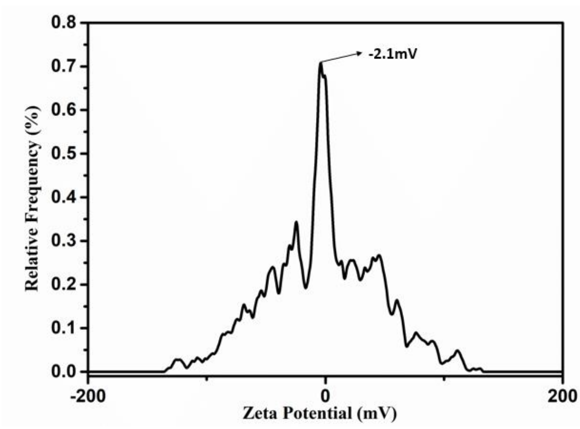

Figure 2. Zeta potential of ZnO nanoparticles

3.2 Particle Size Distribution

The observed particle size was approximately 10 nm. The conductivity of ZnO NPs was found 0.293 mS/cm.

3.3 Zeta Potential Analysis

Figure 2 indicates the results of zeta potential graph of ZnO NPs which were in correspondence with the standard zeta potential range.

3.4 X-ray Diffraction Spectroscopy

In Figure 3 the purity and crystallite size of ZnO were studied by using XRD analysis the diffraction pattern exhibits distinct peak positions at 2θ values 21.52°, 27.05°, 28.48°, 32.99°, 33.80°, 34.30°, 39.51°, and 47.50° whose phase values (hkI) are (114), (400), (022), (217), (009), (224), (325), and (332) corresponding to PDF (00-020-1435) and the evaluated shape was orthorhombic indicating that synthesized material contains $Zn(OH)_2$. According to the Scherrer and Williamson Hall equation, the size of the sample was 1.8 nm, and 11 nm respectively.

3.5 SEM Analysis

Figure 4 shows the high magnification image of high-density ZnO nanoflakes and thickness distribution histogram as determined by using ImageJ software. The thickness of nanoflakes was in the range of 0 to 140 nm (Hanh Nguyen *et al.*, 2021).

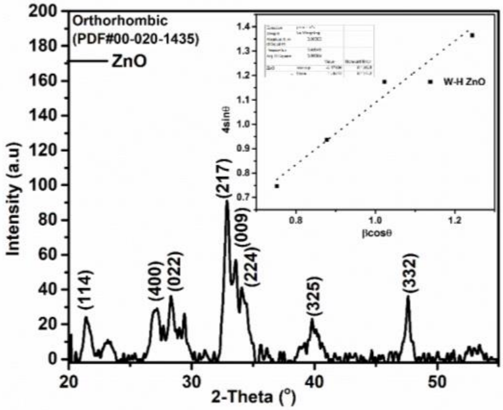

Figure 3. XRD analysis of ZnO nanoparticles

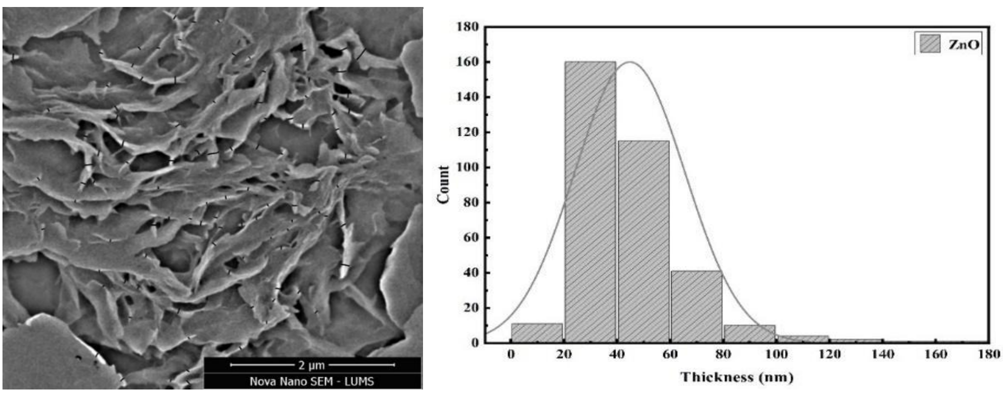

Figure 4. SEM analysis of ZnO nanoparticles

3.6 Photoluminescence Spectroscopy

The effective way to study optical, electronic and photochemical properties of semiconductors like ZnO through PL from Figure 5. A prominent and intense emission peak was visible at 536 nm for ZnO nanoparticles.

3.7 UV-Visible Spectroscopy

From the UV absorbance data, it was concluded that the ZnO NPs synthesized by the green method show maximum absorbance at 271 nm. The optical energy band gap for the ZnO NPs was calculated using the expression proposed by Tauc and Wood (Saleem *et al.*, 2025):

$$(h\nu\alpha) = A\,(h\nu - E_g)^n \qquad \textbf{(5)}$$

where h is Planck's constant, vibrational frequency represented by ν, absorption coefficient is denoted by α, A is a proportionality constant, E_g is bandgap and n with a value of 2 indicates the type of sample transition. Another absorption band of ZnO NPs was observed at 271 nm while absorption band for bulk zinc oxide appeared at 376 nm (Debanath and Karmakar, 2013; Jayachandran *et al.*, 2021). Figure 6 shows the blue shift that comes from the quantum confinement and reduction in the size particles which significantly alters the characteristics of NPs. The confinement of quantum matter can change the bandgap and ease of charge transfer. It also plays a crucial role to improve the covalent bonding and electrostatic interactions which contributes to enhance the sensitivity to biomolecules (Digisu *et al.*, 2024).

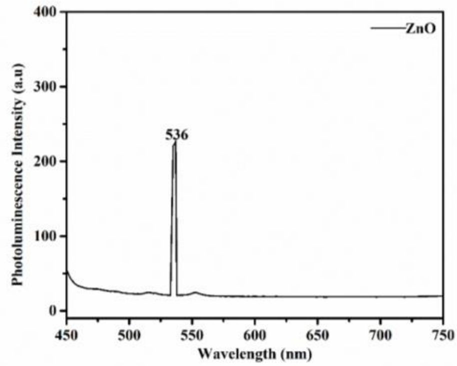

Figure 5. PL spectra of ZnO nanoparticles

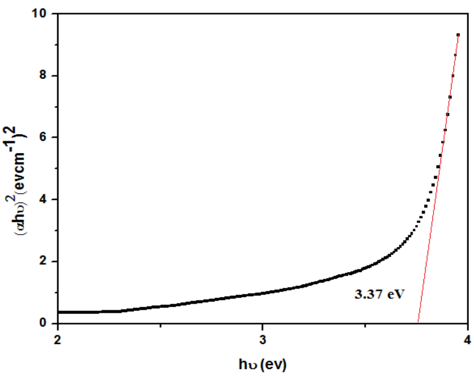

Figure 6. Band Gap of zinc oxide nanoparticles

One of the material's most important characteristic is its refractive index (n) which is closely related to the local field inside the material and the average electronic oxide polarizability of its ions. The relation between the energy gap and the reference index in semiconductors is the subject of the research. The following energy gap-refractive index relationships, derived from Eqs. (6-10) were used to determine the refractive index of semiconductors.

Moss relation

$$n^4E_g = 95ev \qquad \textbf{(6)}$$

where n represents the refractive index and Eg is the energy bandgap of the nanomaterial.

Kumar and Singh's relation

$$n = kE^c_g \qquad \textbf{(7)}$$

Constants K and C have magnitudes of 3.367 and -0.322 respectively.

Harve–Vandamme relation

$$n^2 = 1 + (A / E_g + B)^2 \qquad \textbf{(8)}$$

Where A and B are constants and constant A represents the energy of hydrogen with the value of 13.6 eV while the constant B is taken to be the difference between the UV resonance energy and band gap energy, with a value of 3.47 eV (Imtiaz and Farrukh, 2017).

The bandgap energy may be used directly for the determination of refractive index using Eqs. (7-8).

$$x = 0.2688E_g \qquad \textbf{(9)}$$

$$x = 9.8e^{-n} \qquad \textbf{(10)}$$

where n represents the refractive index. The magnitude of refractive index (n) was evaluated by using Moss, Kumar, and Singh and Harve–Vandamme relations was found to be 2.30, 2.27, and 2.25 respectively, indicating a positive agreement with the refractive index value 2.38 calculated from χ (Perveen and Farrukh, 2017; Abirami *et al.*, 2025).

3.8 Photocatalytic Property of ZnO Nanoparticles

At different irradiation times, the UV-visible spectra of organic dye (methylene blue) solution were obtained using ZnO NPs as shown in Figure 7a. The peak strength was decreased by increasing the irradiation time. The linear relationship of C_t/C_o and ln (C_o/C_t) versus irradiation times are shown in Figure 7b, and c, respectively. Figure 7d shows the degradation efficiency of methylene blue that observed against irradiation time using ZnO NPs. Figure 7a illustrates the proposed method and schematic diagram for photocatalytic breakdown of methylene blue dye using ZnO NPs as shown below:

$$ZnO + h\upsilon \rightarrow ZnO + e^- + h^+ \qquad \textbf{(11)}$$

$$e^- + O_2 \rightarrow O^-_2 \qquad \textbf{(12)}$$

$$h^+ + H_2O \rightarrow OH \qquad \textbf{(13)}$$

$$O_2^- + OH + MB \rightarrow \text{Degradation Product} \qquad \textbf{(14)}$$

Figure 7c depicts that plotting ln (C_o/C_t) versus irradiation time (t) allows the estimation of rate constant for decomposition of MB dye from the slope of straight-line fit. The linear relationship between ln (C_o/C_t) and irradiation time (t) indicates a first order reaction, with a rate constant (k) of 0.0067 min^{-1} for photocatalyst ZnO. On the other hand, Figure 8 shows the GC-MS spectrum of degraded intermediate products and confirms the catalysis of methylene blue. GC/MS chromatogram shows the maximum intensity peak at m/z 44 which elaborates on the presence of the CO_2 compound. The 2-Amino-5-dimethylamino-benzenesulfonic acid anion can be easily identified at 284 m/z using its chemical formula.

The ion abundance ratios suggest that the N-S heterocyclic complex of MB dye was disrupted, as indicated by the presence of

$C_8H_{11}N_2SO_3$. The m/z value is 230 which indicates that the degradation intermediate of 2-Amino-5-dimethylamino-benzenesulfonic acid, with molecular formulas of $C_6H_7NSO_3$ and $C_6H_7NSO_4$, respectively, was attacked by hydroxyl radicals.

Simultaneously, the oxidized 4-Amino-benzenesulfonic acid anion peak at m/z 202.0 has the formula $C_8H_{10}N_2O_2$. The peak appeared at m/z 136 relates to Dimethyl-(4-nitro-phenyl)-amine, $C_6H_{10}N_2O_2$, formed by hydroxyl radical attack on dye molecules' N-S heterocyclic. The peak at 110.0 is p-Dihydroxy benzene, $C_6H_6O_2$, the oxidized result of the benzene ring. The m/z value of 118.0 indicates the tiny molecular products of degradation, similar to succinic acid produced by open-loop benzene ($C_4H_6O_4$). Further analysis showed that the photocatalytic oxidation led to decomposition of conjugated structure of the N-S heterocycle group in MB dye, which is consistent with UV and IR spectrogram data. Figure 9 shows the proposed mechanism for the decomposition of methylene dye.

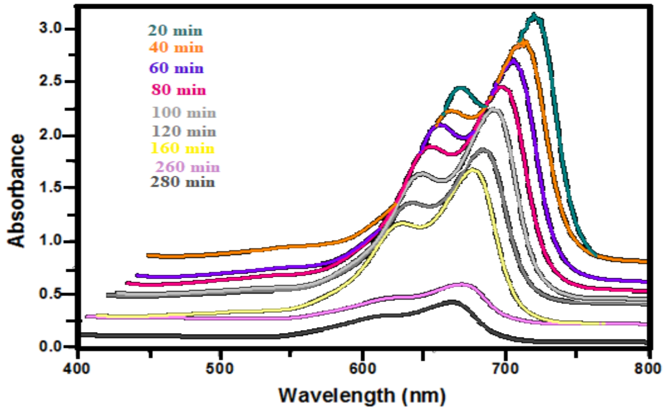

Figure 7a. ZnO nanoparticles-mediated photocatalytic degradation of MB dye

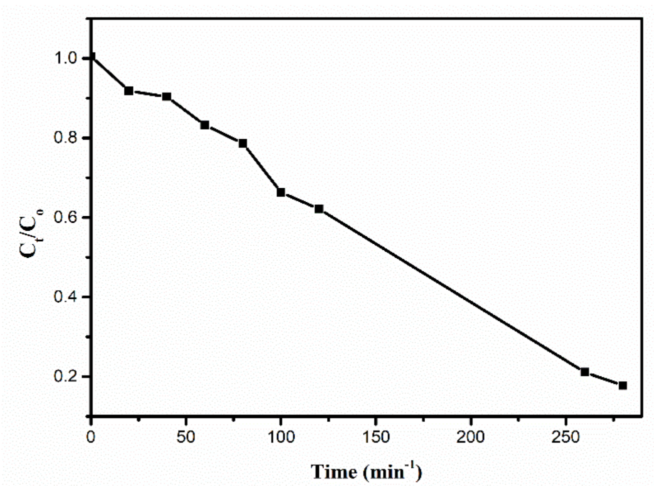

Figure 7b. Degradation of methylene blue dye using UV light as an irradiation source

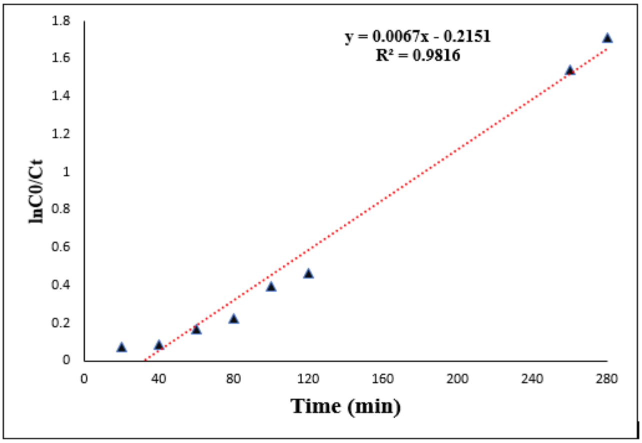

Figure 7c. Photocatalytic activity of ZnO nanoparticles

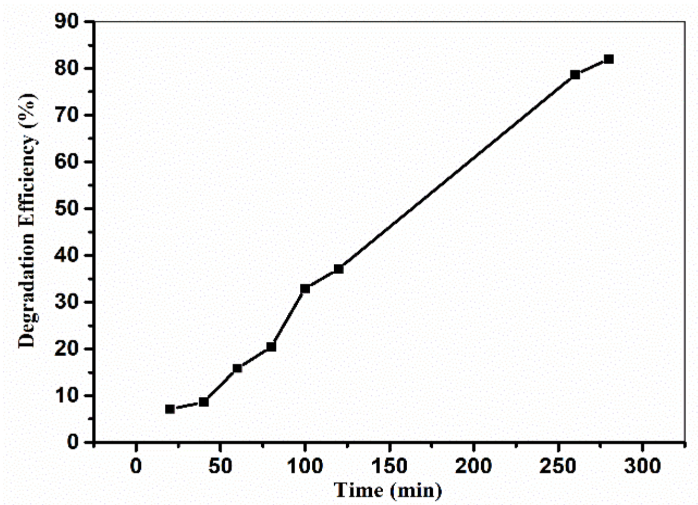

Figure 7d. Methylene blue degradation efficiency of ZnO nanoparticles

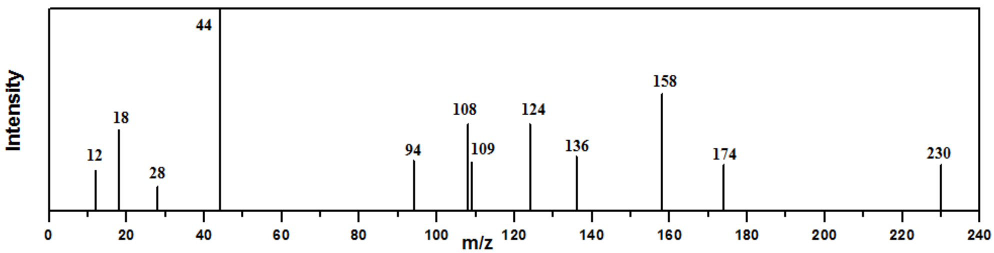

Figure 8. GC-MS chromatogram degradation methylene blue by ZnO nanoparticles at 12.042 retention time

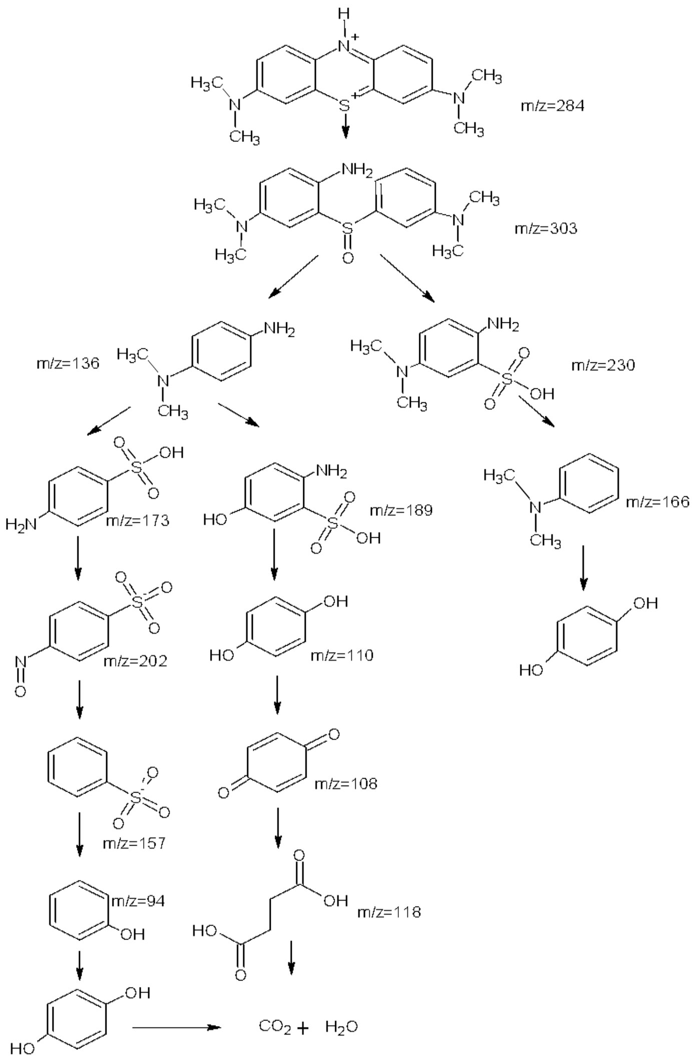

Figure 9. Degradation mechanism of methylene blue by ZnO nanoparticles

3.9 Antibacterial Activity of ZnO Nanoparticles

The highest zone of inhibition was recorded at 17.4 mm against zinc oxide, compared to other doses, while the lowest zone of inhibition was recorded at 10.1 mm. ZnO NPs show mild antibacterial activity, 50% concentrations of NPs remain ineffective to produce an evident zone of inhibition Figure 10. W indicates the *Coriandrum sativum* leaf extract in pure form or 50 % concentration used in activity as shown in Figure 10, 11 and Table 1. However, same trend was recorded for *Staphylococcus aureus* with slight eccentricity in average zone of inhibition which marked slight growth inhibition in Table 1. After antibiotics an evident zone of inhibition was recorded in zinc oxide. From Figure 10, and 11 it is clear that *Staphylococcus aureus* has a greater zone of inhibition as compared to the *Escherichia coli*.

Table 1. Antimicrobial activity measurements against zinc oxide nanoparticles

Nanoparticles	*Staphylococcus aureus*	*Escherichia coli*
	Zone of Inhibition (mm)	
Deionized water (control)	No inhibition	No inhibition
Antibiotics (control)	18.2	17.4
ZnO	17.4	10.9
ZnO 50%	No inhibition	No inhibition
W	10.1	12.4
W 50%	No inhibition	No inhibition

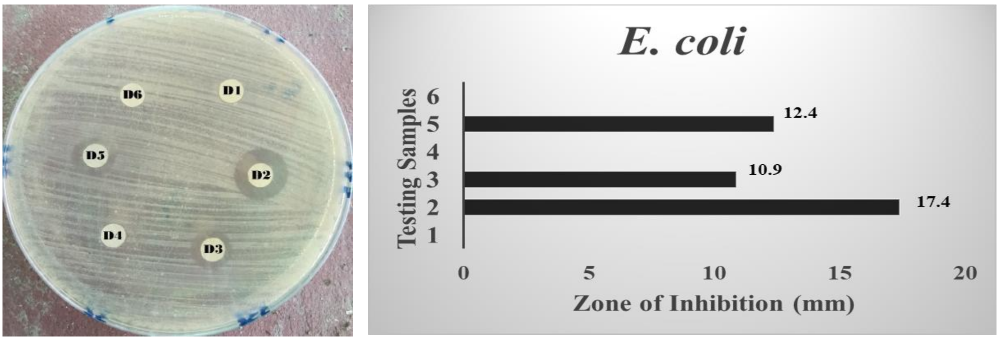

Figure 10. *Escherichia coli* D1-water, D2-Antibiotics (Azithromycin), D3-100% ZnO, D4-50% ZnO, D5-100% W, D6-50% W

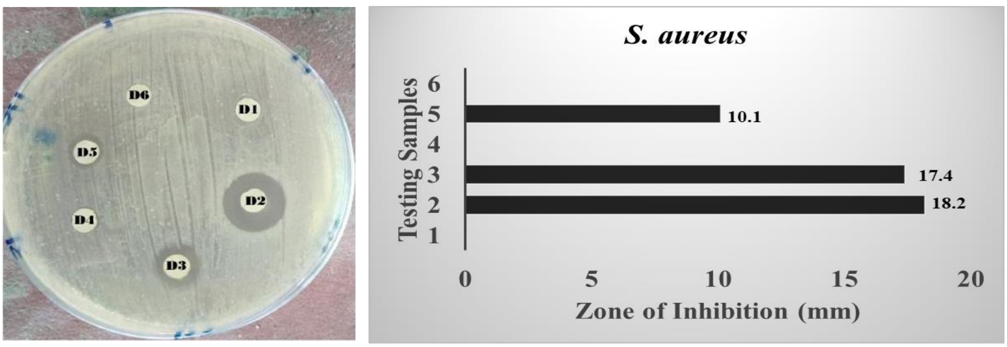

Figure 11. *Staphylococcus aureus* D1-water, D2-Antibiotics (Azithromycin), D3-100% ZnO, D4-50% ZnO, D5-100% W, D6-50% W

4. DISCUSSION

The FTIR results show a strong absorption peak at 3270 cm^{-1} which is due to O-H stretching and occurrence of deformation indicates the adsorption of water molecules onto the metal surface. Similarly, the peak at 1406 cm^{-1} refers to the amine -NH vibration stretch is already reported in literature (Naseer *et al.*, 2020; Sathish *et al.*, 2021). The bands observed at 1564, and 713 cm^{-1} attributes to the Zn-O stretching and vibration frequency, respectively (Chikkanna *et al.*, 2019). Dynamic light scattering (DLS) is widely utilized method for analyzing the particle size distribution of prepared ZnO NPs. This technique also evaluates the dynamic oscillations of light dispersion power that may be caused by the Brownian motion of particles in order to determine the velocity distribution of particle mobility. DLS predicts the particle size perpendicular to the light source and also calculate the hydrodynamic diameter of particles by using Stokes-Einstein equation (Hachenberger *et al.*, 2025). Particles showing zeta values above +30 mV or less than -30 mV, result in stable suspension (Elemike *et al.*, 2018). Water used as a dispersant material for the determination of zeta potential of ZnO NPs. The zeta potential is found to be -2.1 mV shown in Figure 2. The obtained value indicates the presence of repulsive forces between particles and enhances the structural stability. The presence of a hydroxide phase rather than crystalline ZnO in the X-ray Diffraction Spectroscopy is common in green synthesis routes, where $Zn(OH)_2$ serves as a precursor that converted to ZnO later under thermal treatment or further processing. Therefore, the presence of $Zn(OH)_2$ supports the successful initial synthesis step toward ZnO nanoparticle formation and does not diminish the relevance or potential of the method. The peak at 536n for ZnO particles in Photoluminescence Spectroscopy might indicate the presence of defects like singly ionized oxygen vacancies. Green synthesized ZnO has more surface oxygen vacancies as indicated by the green emission band's PL intensity, which is higher in ZnO flowers. According to several recent studies, vacancies caused by surface oxygen defects can have a major impact on ZnO nanostructures and photocatalytic applications (Donkadokula *et al.*, 2020).

It has also been observed that the intermediate photo products or dye reacts with ·OH free radicals which leads to discoloration of methylene blue dye solution (Ismail *et al.*, 2019). On the other hand, particle size of synthesized metal oxides, their morphological structure and charge properties also play a crucial role for discoloration of dyes (Chand *et al.*, 2020). Thus, the color or organic dyes could be effectively degraded by the size controlled ZnO NPs with surface charge. İn recent studies, Kumar et al. reported that organic dyes may be degraded more efficiently with increases in time using green or biosynthesized metal NPs (Wang *et al.*, 2018). Similarly, at the specified conditions, ZnO NPs (prepared via green synthesis method) have a high potential towards methylene blue dye degradation up to 82 %. The degradation of methylene blue dye is caused by visible changes in solution color from dark blue to colorless when UV radiation is utilized as an UV light irradiation source. The increasing the electron density of sulfhydryl, free hydroxyl radicals gain a high potential to break down the conjugated structure of N-S heterocycle during the photocatalytic oxidation of methylene blue, causing it to degrade to 2-Amino-5-dimethylamino-benzenesulfonic acid anion and Dimethyl-(4-nitro-phenyl)-amine. Basically, hydroxyl radicals transformed the dimethyl-(4-nitrophenyl) amine to p-dihydroxybenzene.

The anion 2-Amino-5-dimethylamino-benzenesulfonic acid continues to break down into 4-Amino-benzenesulfonic acid and 2-Amino-5-dimethylamino-benzenesulfonic acid.

The oxidation of 4-Amino-benzenesulfonic acid produced a 4-Nitro-benzenesulfonic acid anion. Ultimately, the 4-Nitro-benzenesulfonic acid anion was directly targeted and destroyed into CO_2 and H_2O through several reactions (Wang *et al.*, 2018).

ZnO NPs also have the potential to damage the bacterial membranes of *Staphylococcus aureus*, likely through the generation of reactive oxygen species, including superoxide and hydroxyl radicals as well. Additionally, the surface of ZnO NPs has a negative zeta potential and is dependent upon the surface characteristics of certain microorganisms. Furthermore, the antibacterial activity is said to be influenced by the kind of surfactant utilized as well as the concentration of ZnO NPs. Additionally, ZnO NPs may have caused the bacterial cell membrane to rupture and the cytoplasmic contents to extrude, ultimately leading to the bacterium's demise. On the basis of various research studies, it can be concluded that ZnO NPs may have inhibited bacterial development of *Staphylococcus aureus* better than *Escherichia coli* because the ZnO NPs contain a negative charge and the *Staphylococcus aureus* is gram-positive so its membrane is easily ruptured as compared to *Escherichia coli*.

5. CONCLUSIONS

ZnO NPs were successfully synthesized using *Coriandrum sativum* leaf extract, achieving 82% degradation of MB dye under UV light over 280 minutes, and notable antibacterial activity, which is attributed to their physicochemical properties. These findings highlight the dual functionality of *Coriandrum sativum* synthesized ZnO NPs as efficient photocatalysts and antibacterial agents, suggesting their potential for wastewater treatment and antimicrobial applications. Future work may focus on scale-up synthesis and testing against a broader range of pathogens.

Conflict of Interest

No conflicts of interest need to be addressed.

Author Contributions

Bakhtawar Sajjad: synthesis and experimentation, Humayun Ajaz: designing methodology, supervision and interpretation of results, Shaista Ali: characterization, interpretation, Muhammad Mudassar: interpretation and editing, Atif Yaqub: interpretation and supervision of data, Sarwar Allah Ditta: software and resources, Sharafat Ali: experimentation and interpretation.

Ethics approval and Informed Consent

Not required

Availability of data

The data used to support the findings of this study is included within the manuscript.

Funding

No funding was received.

REFERENCES

Abdullah, F., Bakar, N. A. and Bakar, M. A. 2022. Current advancements on the fabrication, modification, and industrial application of zinc oxide as photocatalyst in the removal of organic and inorganic contaminants in aquatic systems. *Journal of hazardous materials,* 424:127416.

Abirami, S., Kumar, E. and Vigneshwaran, B. 2025. Investigation of CeVO 4 content on the structural and thermal properties of PANI/CeVO 4 nanocomposites. *Ionics,* 31:3021-3036.

Ahmad, S., Aadil, M., Ejaz, S. R., Akhtar, M. U., Noor, H., Haider, S., Alsafari, I. A. and Yasmin, G. 2022. Sol-gel synthesis of nanostructured ZnO/SrZnO2 with boosted antibacterial and photocatalytic activity. *Ceramics International,* 48:2394-2405.

Aldeen, T. S., Mohamed, H. E. A. and Maaza, M. 2022. ZnO nanoparticles prepared via a green synthesis approach: Physical properties, photocatalytic and antibacterial activity. *Journal of Physics and Chemistry of Solids,* 160:110313.

Altaf, S., Ijaz, H., Haider, J., Naz, M., Aqeel, M., Ul-Hamid, A., Ikram, M., Zulfiqar, S., Ditta, S. and Shahbaz, A. 2020. Influence of various transition metals incorporated into tellurium used as antimicrobial agent and textile dye degrader. *Applied Nanoscience,* 10:4241-4254.

Chan, Y. Y., Pang, Y. L., Lim, S. and Chong, W. C. 2021. Facile green synthesis of ZnO nanoparticles using natural-based materials: Properties, mechanism, surface modification and application. *Journal of environmental chemical engineering,* 9:105417.

Chand, K., Cao, D., Eldin Fouad, D., Hussain Shah, A., Qadeer Dayo, A., Zhu, K., Nazim Lakhan, M., Mehdi, G. and Dong, S. 2020. Green synthesis, characterization and photocatalytic application of silver nanoparticles synthesized by various plant extracts. *Arabian Journal of Chemistry,* 13:8248-8261.

Chikkanna, M. M., Neelagund, S. E. and Rajashekarappa, K. K. 2019. Green synthesis of zinc oxide nanoparticles (ZnO NPs) and their biological activity. *SN Applied Sciences,* 1:117.

Debanath, M. and Karmakar, S. 2013. Study of blueshift of optical band gap in zinc oxide (ZnO) nanoparticles prepared by low-temperature wet chemical method. *Materials letters,* 111:116-119.

Digisu, A. W., Yaebyo, A. B., Kebede, W. L., Kebede, D. Y. and Molla, D. K. 2024. Biogenic synthesis, optimization, and characterization of zinc oxide nanoparticles using *Rumex abyssinicus Jacq* root extract for antioxidant and antibacterial activities. *Results in Chemistry,* 12:101857.

Donkadokula, N. Y., Kola, A. K., Naz, I. and Saroj, D. 2020. A review on advanced physico-chemical and biological textile dye wastewater treatment techniques. *Reviews in environmental science and bio/technology,* 19:543-560.

Doubi, Y., Hartiti, B., Siadat, M., Labrim, H., Fadili, S., Tahri, M. and Thevenin, P. 2022. The high impact of solution flow rate on optical properties of TiO2 thin layers for optoelectronic applications. *Crystal Research and Technology,* 57:2200129.

Elemike, E. E., Onwudiwe, D. C., Abiola, O. K. and Ibe, K. A. 2018. Surface characterisation and reaction kinetics of silver nanoparticles mediated by the leaf and flower extracts of French marigold (*Tagetes patula*). *IET nanobiotechnology,* 12:957-962.

Hachenberger, Y. U., Krause, B. C., Kriegel, F. L., Reichardt, P., Tentschert, J., Jungnickel, H., Bierkandt, F. S., Laux, P., Panne, U. and Luch, A. 2025. Developing a multi-method approach for understanding cellular uptake and biological response: Investigating co-exposure of macrophage-like differentiated THP-1 cells to Al_2O_3 and CeO_2 nanoparticles. *Molecules,* 30:1647.

Haleem, A., Shafiq, A., Chen, S.-Q. and Nazar, M. 2023. A comprehensive review on adsorption, photocatalytic and chemical degradation of dyes and nitro-compounds over different kinds of porous and composite materials. *Molecules,* 28:1081.

Hanh Nguyen, T., Pham, X. M., Nguyen, T. N., Thi, N. H., DangThi, T. A., Tran, Q. V., Vu, A. T., Hoang, M. H. and Nguyen, T. V. 2021. Preparation of ZnO nanoflakes and assessment of their removal of HCN, NO_2 and SO_2 toxic gases. *International Journal of Materials Research,* 112:10-16.

Hussain, A., Zahid, A., Ali, S., Khalid, N., Ashraf, A., Latif, A., Farrukh, M. A. and Jabeen, M. 2024. Enhancing the photocatalytic efficiency of green synthesized MoO_3 and MnO nanoparticles by making heterojunction with graphene oxide. *Journal of the Taiwan Institute of Chemical Engineers,* 163:105642.

Imtiaz, A. and Farrukh, M. A. 2017. Influence of CdS dopant on oxygen vacancies and

Ce^{3+} formation in CeO_2–ZnO nanocomposites: structural, optical and catalytic properties. *Journal of Materials Science: Materials in Electronics,* 28:2788-2794.

Ismail, M., Akhtar, K., Khan, M. I., Kamal, T., Khan, M. A., M. Asiri, A., Seo, J. and Khan, S. B. 2019. Pollution, toxicity and carcinogenicity of organic dyes and their catalytic bio-remediation. *Current Pharmaceutical Design,* 25:3645-3663.

Javed, M., Qamar, M. A., Shahid, S., Alsaab, H. O. and Asif, S. 2021. Highly efficient visible light active Cu–ZnO/SgC_3N_4 nanocomposites for efficient photocatalytic degradation of organic pollutants. *RSC advances,* 11:37254-37267.

Jayachandran, A., Aswathy, T. and Nair, A. S. 2021. Green synthesis and characterization of zinc oxide nanoparticles using *Cayratia pedata* leaf extract. *Biochemistry and Biophysics Reports,* 26:100995.

Kamarajan, D., Anburaj, B., Porkalai, V., Muthuvel, A., Nedunchezhian, G. and Mahendran, N. 2022. Green synthesis of ZnO nanoparticles and their photocatalyst degradation and antibacterial activity. *Journal of Water and Environmental Nanotechnology,* 7:180-193.

Karthik, K., Raghu, A., Reddy, K. R., Ravishankar, R., Sangeeta, M., Shetti, N. P. and Reddy, C. V. 2022. Green synthesis of Cu-doped ZnO nanoparticles and its application for the photocatalytic degradation of hazardous organic pollutants. *Chemosphere,* 287:132081.

Khan, I., Saeed, K., Zekker, I., Zhang, B., Hendi, A. H., Ahmad, A., Ahmad, S., Zada, N., Ahmad, H. and Shah, L. A. 2022. Review on methylene blue: its properties, uses, toxicity and photodegradation. *Water,* 14:242.

Madhumitha, G., Fowsiya, J., Gupta, N., Kumar, A. and Singh, M. 2019. Green synthesis, characterization and antifungal and photocatalytic activity of *Pithecellobium dulce* peel–mediated ZnO nanoparticles. *Journal of Physics and Chemistry of Solids,* 127:43-51.

Naseer, M., Aslam, U., Khalid, B. and Chen, B. 2020. Green route to synthesize zinc oxide nanoparticles using leaf extracts of *Cassia fistula* and *Melia azadarach* and their antibacterial potential. *Scientific Reports,* 10:9055.

Osuntokun, J., Onwudiwe, D. C. and Ebenso, E. E. 2019. Green synthesis of ZnO nanoparticles using aqueous *Brassica oleracea* L. var. italica and the photocatalytic activity. *Green chemistry letters and reviews,* 12:444-457.

Perveen, S. and Farrukh, M. A. 2017. Influence of lanthanum precursors on the heterogeneous La/SnO_2–TiO_2 nanocatalyst with enhanced catalytic activity under visible light. *Journal of Materials Science: Materials in Electronics,* 28:10806-10818.

Rueda-Marquez, J. J., Levchuk, I., Ibañez, P. F. and Sillanpää, M. 2020. A critical review on application of photocatalysis for toxicity reduction of real wastewaters. *Journal of Cleaner Production,* 258:120694.

Sadiq, H., Sher, F., Sehar, S., Lima, E. C., Zhang, S., Iqbal, H. M., Zafar, F. and Nuhanović, M. 2021. Green synthesis of ZnO nanoparticles from *Syzygium Cumini* leaves extract with robust photocatalysis applications. *Journal of Molecular Liquids,* 335:116567.

Saleem, M. H., Ali, S., Farrukh, M. A. and Gillani, S. S. A. 2025. Investigating the properties of cubic and hexagonal Nd_2O_3 nanoparticles for optics & energy storage material: Experimental and DFT approach. *Solid State Communications,* 397:115836.

Sathish, P., Dineshbabu, N., Ravichandran, K., Arun, T., Karuppasamy, P., SenthilPandian, M. and Ramasamy, P. 2021. Combustion synthesis, characterization and antibacterial properties of pristine ZnO and Ga doped ZnO nanoparticles. *Ceramics International,* 47:27934-27941.

Singh, A., Sikarwar, S., Verma, A. and Yadav, B. C. 2021. The recent development of metal oxide heterostructures based gas sensor, their future opportunities and challenges: a review. *Sensors and Actuators A: Physical,* 332:113127.

Wang, X.-q., Han, S.-f., Zhang, Q.-w., Zhang, N. and Zhao, D.-d. 2018. Photocatalytic oxidation degradation mechanism study of methylene blue dye wastewater with GR/iTO_2. *MATEC Web of Conferences,* 238:03006.

Weldegebrieal, G. K. 2020. Synthesis method, antibacterial and photocatalytic activity of ZnO nanoparticles for azo dyes in wastewater treatment: A review. *Inorganic Chemistry Communications,* 120:108140.